PROCEEDINGS OF SPIE

SPIEDigitalLibrary.org/conference-proceedings-of-spie

Development of the 4-telescope photonic nuller of Hi-5 for the characterization of exoplanets in the mid-IR

A. Sanny, S. Gross, L. Labadie, D. Defrère, A. Bigioli, et al.

A. Sanny, S. Gross, L. Labadie, D. Defrère, A. Bigioli, R. Laugier, C. Dandumont, M. Withford, "Development of the 4-telescope photonic nuller of Hi-5 for the characterization of exoplanets in the mid-IR," Proc. SPIE 12183, Optical and Infrared Interferometry and Imaging VIII, 1218316 (26 August 2022); doi: 10.1117/12.2628903

SPIE.

Event: SPIE Astronomical Telescopes + Instrumentation, 2022, Montréal, Québec, Canada

Development of the 4-telescope photonic nuller of Hi-5 for the characterization of exoplanets in the mid-IR

A. Sanny[a,b], S. Gross[a], L. Labadie[b], D. Defrère[c], A. Bigioli[c], R. Laugier[c], C. Dandumont[c], and M. Withford[b]

[a]MQ Photonics Research Centre, School of Mathematical and Physical Sciences, Macquarie University, NSW 2109, Australia
[b]I. Physikalisches Institut, Universität zu Köln, Zülpicher Str. 77, 50937 Köln, Germany
[c]Institute of Astronomy, KU Leuven, Celestijnenlaan 200D, 3001, Leuven, Belgium

ABSTRACT

A small-footprint 4-telescope photonic beam combiner is at the heart of the Hi-5 instrument, the high-contrast VLTI visitor instrument focusing on the detection and characterization of young exoplanets in the mid-infrared L' band. Hi-5 implements the technique of nulling interferometry to efficiently suppress the strong stellar radiation of the central source and enhance the detection of the nearby faint planetary signal. Based on the "Double Bracewell" architecture, the photonic nulling beam combiner is designed around three cascaded achromatic directional couplers with 50/50 coupling ratios. This allows the nulled signals of the first two couplers to be cross-combined with a third central combiner, which produces two conjugated asymmetric transmission maps projected onto the sky. Each individual telescope beam passes first through a side-step to suppress uncoupled stray-light. The corresponding flux is then sampled by an asymmetric Y-junction to provide a simultaneous photometric channel for the estimation of the self-calibrated nulls. We report here on the prototyping phase of the Hi-5 4-telescope photonic beam combiner that is manufactured by ultrafast laser inscription in a Gallium-Lanthanum-Sulphide (GLS) glass substrate, which exhibits high transparency in the L' band of interest. Using our 2-beam spectro-interferometric lab bench, we measure the throughput of the beam combiners, the chromatic and broadband coupling ratios in the 3.6-3.9 µm range for the couplers and the Y-junctions, as well as the broadband interferometric properties of these 4-telescope mid-infrared photonic beam combiners.

Keywords: Nulling, Interferometry, Astrophotonics, Integrated Optics, Optical/Infrared Instrumentation

1. INTRODUCTORY

Hi-5 is a proposed high contrast imager for the VLTI instrument ASGARD[1] to perform self-calibrated simultaneous nulling interferometry using integrated photonics in the mid-infrared L' (3.5-4.0 µm) band. This instrument is a successor of other 4-telescope interferometers like PIONIER (H band), GRAVITY (K band), and MATISSE (L, M, and N).

Nulling interferometry is a method to detect and investigate exoplanets or faint objects near any bright astronomical object, such as a star, by suppressing the bright incoming on-axis signal from the prime source using destructive interference. Bracewell proposed this concept for a rotating 2-telescope system.[2] Several decades later, Angel & Woolf proposed a modified version for a linearly cascaded 4-telescope system.[3] Both concepts were based on bulk optics. However, integrated optics have emerged as the platform of choice to replace bulk optics for beam combination. Integrated optics use single-mode waveguides to provide spatial filtering of the incoming light from the telescope. They are compact in size and exhibit higher mechanical stability. An integrated optic implementation of the beam combination scheme proposed by Angel & Woolf was demonstrated by Errmann *et al.*[4] for monochromatic visible light (633 nm). Improving those techniques in experiment, the aim of the Hi-5

Further author information: (Send correspondence to L. Labadie.)
L. Labadie: E-mail: labadie@ph1.uni-koeln.de, Telephone: +49 221 470 3493
A. Sanny: E-mail: ahmed@ph1.uni-koeln.de, Telephone: +49 221 470 3548

Optical and Infrared Interferometry and Imaging VIII, edited by Antoine Mérand, Stephanie Sallum, Joel Sanchez-Bermudez,
Proc. of SPIE Vol. 12183, 1218316 · © 2022 SPIE · 0277-786X · doi: 10.1117/12.2628903

is to develop an integrated optic 4-telescope beam combiner to perform nulling interferometry in the mid-IR (L' band) that incorporates taps to simultaneously obtain photometric signals.

The astronomical L' band is significant for discovering, observing, and characterising exozodiacal disks and young giant planets down to the snow line, which is a possible water-ice forming region of a planetary system.[5] This mid-infrared wavelength band is also favorable for performing nulling interferometry compared to the K and N bands. A small phase error between two beams, caused by the fringe tracking or stabilization quality, can shift the dark fringe to a non-null on-axis transmission. For a fringe tracker that stabilized down to a balance phase error, the K band's fractional phase error is higher than the L band due to the K band's shorter wavelength.[6] Compared to the N band, L' band can provide higher angular resolution and offer limited residual thermal background error compared to the N band (such as Keck Interferometric Nuller) due to the short wavelength regime.[7]

Therefore, we have been developing a 4-telescope photonic beam combiner for nulling interferometry using the ultrafast laser inscription (ULI) technique in a substrate which exhibits high transparency in the L' band of interest.

This proceeding paper will present a characterisation of the prototype Hi-5 4-telescope photonic chip that is manufactured at Macquarie University, Australia and characterized using a 2-beam spectro-interferometric lab bench at the University of Cologne, Germany, to understand the functional properties of the nulling combiners in the realm of developing the final component for on-sky operation.

2. REQUIREMENTS OF 4T BEAM COMBINER FOR THE HI-5

The required integrated optics waveguide chip for the Hi-5 instrument features four inputs to simultaneously accept light from 4 telescopes of the VLT array. All 4 inputs undergo a S-bend to the side for suppression of uncoupled stray light.[8] Following the S-bend, there are 4 achromatic Y-junctions to tap off a fraction of the light for the photometry channels that facilitate full self-calibration of the nulled output signals.[5] The interferometric beam combination section first combines two pairs of inputs using 50/50 directional couplers (DC), as shown in Fig.1, labelled with DC1 and DC2. The two cross-coupled outputs of the first pair of directional couplers are further combined in a third 50/50 directional coupler, labelled with CC in Fig.1. This creates two nulled signals as outputs I2 and I3, as shown in 1. The bar signals of DC1 and DC2, which are not crossed coupled, propagate as two individual bright outputs, I1 and I4. The splitting ratios of the three couplers need to be spectrally flat to meet the Hi-5 requirements for a deep suppression of the star light.

Furthermore, various loss contribution, coupling efficiency to single-mode waveguides, differential birefringence, and chromatic differential dispersion in polychromatic and unpolarized environments are essential considerations for achieving a strong instrumental null or extinction ratio.[9,10]

In brief, Table 1 contains a summary of the basic requirements.

Table 1. Requirements for the 4T nulling beam combiner

Requirements	Parameters
Wavelength Range	3.5-4.0 μm
Telescope Inputs	4
Photometry Outputs	4
Interferometry Outputs	4
Split between Photometry and Interferometry	20/80
Coupling Ratios (Bar/Cross)	50/50
Throughput	$> 50\%$
Operating Temperature	> 40°K

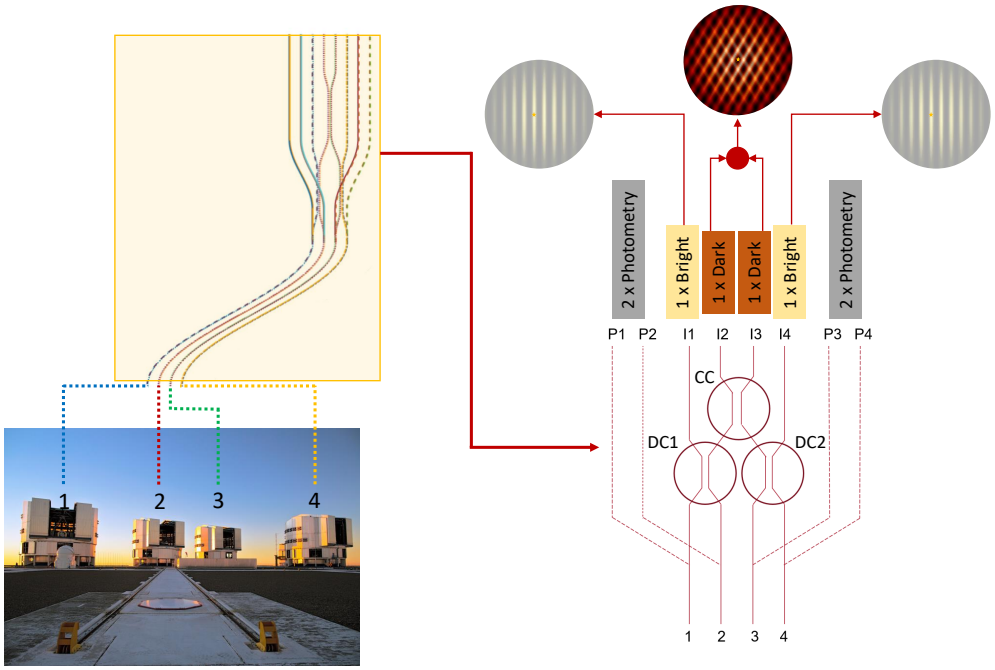

Figure 1. The left top corner displays a schematic layout of the 4T beam combiner, and the bottom image shows the connections between the four inputs of the nulling device and 4 telescopes of VLTI. It also illustrates the S-bends and how the light is guided to beam combination section of the integrated optic chip. Another simplified sketched diagram of the nulling beam combiner is presented on the right side to reveal the internal elements. The photometry signals from each input are separated by the Y-junctions and routed to the outpus P1, P2, P3, and P4. The remaining signals from the Y-junctions propagate through the interferometry section of the chip and produce four interferometric outputs – I1, I2, I3, and I4. From the four interferometric outputs, I1 and I4 produce bright signals and I2 and I3 produce isolated nulled signals.

3. MANUFACTURING TECHNIQUE

The ultrafast laser inscription (ULI) technique is used for manufacturing the integrated optics 4T nulling beam combiner. The core principle of this technique is to change the refractive index of the substrate material permanently by using a tightly focused, high-intensity laser beam. Translating the substrate material against a tightly focused laser beam creates a refractive index modification, that if positive in sign can act as a waveguide. Several factors such as laser pulse duration, pulse repetition rate, and laser fluence determine the size, shape and magnitude of the index change inside the substrate material. A general discussion of ULI was presented by Gross and Withford,[11] Gretzinger *et al.*,[12] and Osellame *et al.*[13]

The choice of substrate materials transparent in the mid-infrared range is limited. Gallium Lanthanum Sulphide (GLS) of the chalcogenide glasses family exhibits 0.5 to 10 m transparency range. Consequently, GLS has been used as the substrate material for developing the optical chip for the Hi-5 due to its broad transparency window in thermal mid-infrared regime, which covers the L' band, and its response with a positive refractive index change to femtosecond laser irradiation. This enables the fabrication high quality waveguides.[12]

Rodenas *et al.*[14] and Arriola *et al.*[15] demonstrated Y-splitters and directional couplers (DC) in GLS using ULI. Tepper *et al.*[16] characterized similar components and demonstrated high broadband interferometric contrasts, small spectral phase distortion, and 30% to 60% throughput for L, L' and M bands. These findings influenced the selection of GLS as a suitable substrate material for the desired 4T nulling devices. The fabrication recipe for manufacturing the 4T beam combiners in GLS is based on the work done by Gretzinger *et al.*,[12] which combines the cumulative heating regime with the multiscan technique to produce single-mode optical waveguides. The work showed that propagation losses at 4 µm as low as 0.22 ± 0.02 dB/cm with < 0.1 dB/cm polarization

dependency can be achieved. Cosine S-bends have a negligible bending loss in a window (3.6 - 4.2 µm) for bend radii > 40 mm, and the work also demonstrates directional couplers with 50/50 splitting ratio. Based on these results a prototype integrated optic beam combiner was fabricated in GLS glass for Hi-5.

The manufactured chip contains various photonic elements, including the 4T beam combiners, multiple S-bends, individual directional couplers as reference and Y-junctions. All waveguides are written as triplet or triple tracks to ensure low loss guiding.[12] A 49 mm long GLS glass piece was used as substrate. The writing depth from the surface is 180 µm. To fit more devices, the inscription was performed from both sides, top and bottom, of the GLS glass substrate, further on designated side A and side B. Side A contains 7×2 4T-beam combiners with linearly arrayed input and outputs where the pitch between waveguides is 125 µm. The amplitudes of the internal S-bends are 1.8 mm with 45 mm radius of curvature. The photometry signals are also separated with 45 mm radius of curvature S-bends and the interferometry signals employ 50 mm radius of curvature. The right waveguide of the directional couplers features a change in propagation constant/effective index to introduce asymmetricity inside the coupler for creating achromatic splitting. The three directional couplers of each combiner exhibit equal interaction length. However, each individual 4T beam combiner features directional couplers with incrementialy longer interaction lengths. The interaction lengths gradually increase from $l = 5.0$ mm to $l = 6.2$ mm in steps of 0.2 mm for each beam combiner. The writing order of the three individual modifications of each waveguides are not identical. DC1 and DC2 are written in the same order called inside out, where the first track written is closest to the centre of the coupling region. The second and third are gradually written outward. The central combiners (CC) are fabricated in the opposite order due to the geometry of the beam combiner and resulting writing sequence. The chip consists of a block of reference 2×2 directional couplers on side B, where the difference between couplers is the interaction length, starting from $l = 4.0$ mm and ending at $l = 7.0$ mm. All directional couplers feature a distance from the centre of the waveguide to the centre of the adjacent waveguide of 21 µm in the coupling region.

4. CHARACTERISATION SETUP

Depending on the experimental requirements, we have characterized the fabricated photonic chip against a supercontinuum laser source (SCS) and a blackbody thermal source (BBS). Both sources are used in combination with a L' bandpass filter. The corresponding normalized spectra are presented in Fig.2. Both sources generate signals at the central wavelength of the L' band at 3.75 µm but lack flux towards the short wavelength limit of the L' band.

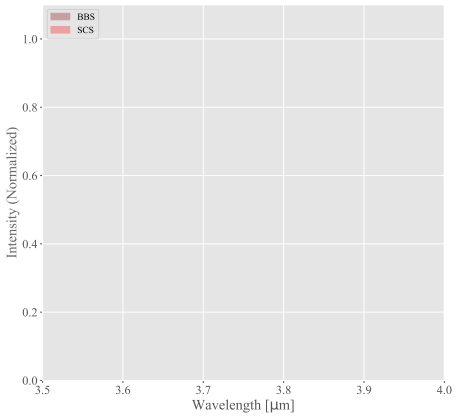

Figure 2. Normalized emission spectra of the SCS and BBS after the L' bandpass filter.

The experimental setup is illustrated in Fig.3. A single-mode infrared-transparent fiber (InF3, 2-5.5 µm, 0.26NA) with a 9 µm core diameter passes the signal from the source to the optical bench. The Michelson interferometer produces two independent light beams that are injected into the integrated optics components

using a 50 mm focal length injection lens. The beam combiners are mounted on a 5-axis stage. Using another 50 mm lens the output light is projected onto an IR camera sensitive in the 2-5 µm range with 30×30 µm pixels (InfraTec-IRBIS). The detector is operated between 50 Hz and 250 Hz frame rate. The delay-line enables control of the relative path difference between two beams in the setup. This test bench can be used as a Fourier transform spectrometer to perform chromaticity-related spectroscopic measurements. In this case, a reference HeNe laser of known wavelength of 3 .39 µm is used for metrology of the delay line in conjunction with either the black-body or supercontinuum sources.

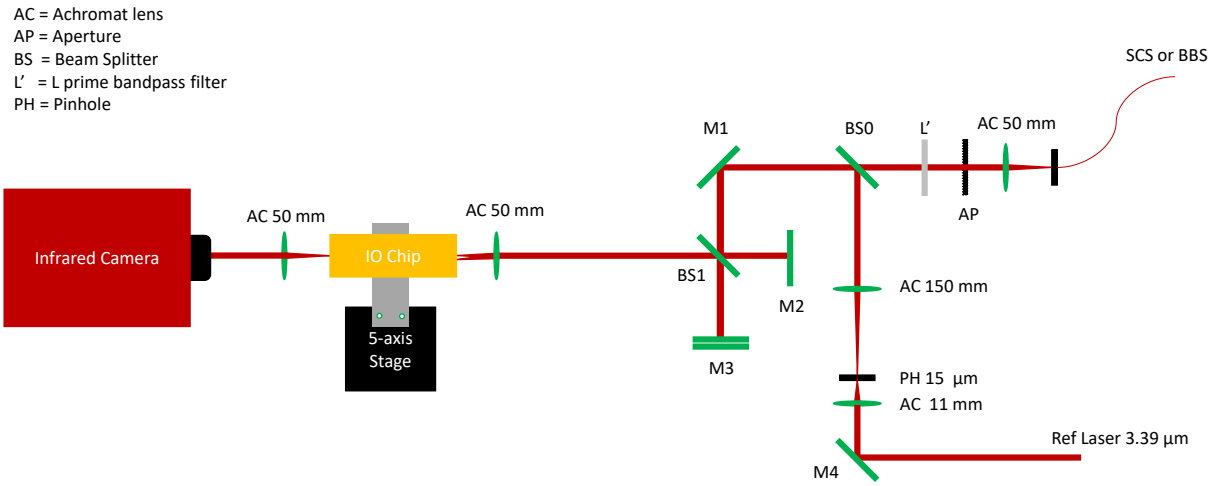

Figure 3. Schematic diagram of the experimental test bench – source (SCS or BBS) propagates to the test bench using a fibre cable and passes through various optical elements. M1, MS1, M2, and delay line mirror M3 are placed to perform Michelson interferometry. A metrology signal (Ref. Laser) for calibration is introduced to the Michelson interferometer via BS0.

5. CHROMATIC CHARACTERISATION

The splitting characteristics of the Y-junctions and directional couplers (DC1, DC2, and CC) were measured by using the test bench as a Fourier transform spectrometer. For this purpose the two beams from the Michelson interferometer were collinear and sequentially injected into all four inputs of a given beam combiner. This resulted in four output spots on the detector, one from the photometry channel and the other three from the interferometry outputs. The intensities were recorded while the delay line was moving, producing an interferogram for each output. Simultaneously, another interferogram was recorded based on the reference laser that was injected into a neighbouring waveguide. The monochromatic interferogram of the metrology laser was used to calibrate the position of the delay line and thus the wavelength axis. The chromatic splitting ratios were derived by applying the Fast Fourier Transform (FFT) using the following formulas – for identifying the chromatic splitting between photometry (P) and interferometry (I) by Y-junction, P/(P+I) and I/(P+I). The splitting ratios for individual directional couplers are calculated as Bar/(Bar+Cross) and Cross/(Bar+Cross), where Bar refers to the light that stays inside the waveguide in which light was injected into and Cross for the light that has coupled to the neighbouring waveguide. An example of these chromatic splitting characteristics of a nulling beam combiner is shown in Fig.4.

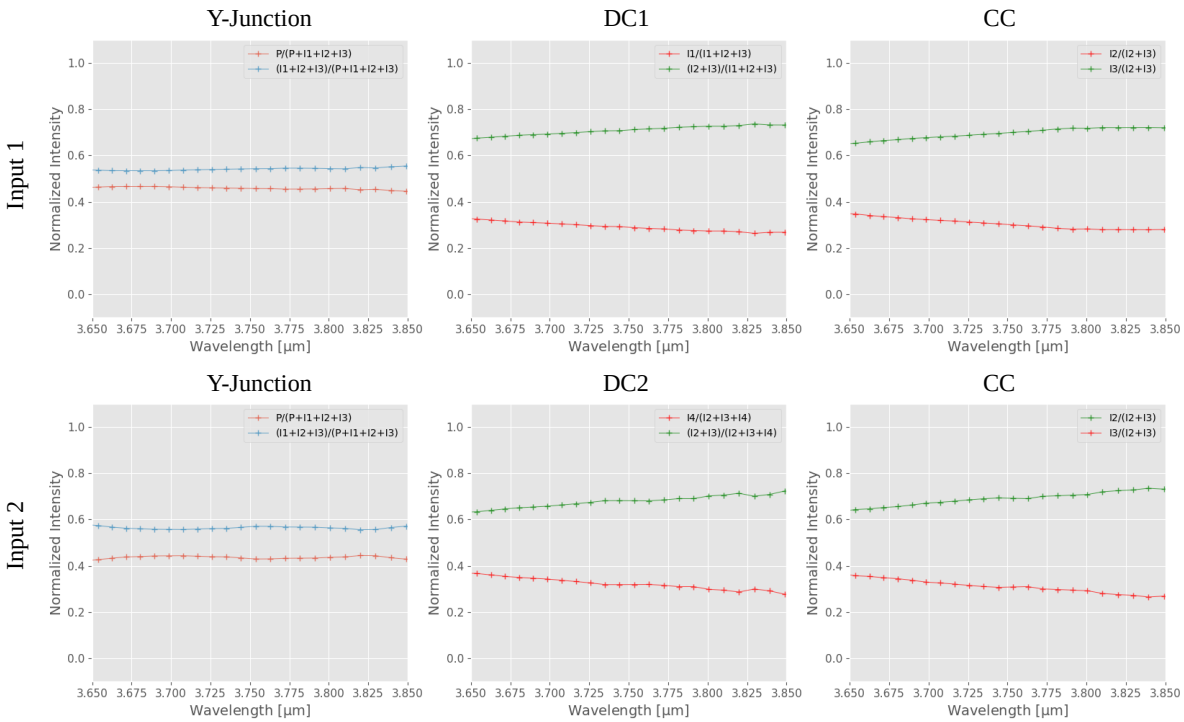

Figure 4. Chromatic splitting ratios of a 4T beam combiner. The interaction length of the directional couplers is 5.6 mm. The top row shows the chromatic behaviour for light injected into input 1, while the bottom row is for injection into input 4, respectively. The left column indicates the spectral splitting between photometry (red colour) and interferometry (blue colour) channel by the first and fourth Y-junction in the chip. The first plot of the central column displays the splitting ratios of DC1, while the second plot indicates DC2. The right column presents the splitting behaviour of the CC. Bar and cross splitting ratios of the couplers are shown in red and green colour, respectively.

The characterization suggests that the average splittings between all the photometry and interferometry signals of the 4T beam combiners at 3.75 μm is 37/56 with a variance of ±11% / ±7%. The splitting is off from the desired 20/80 for the photometry. Increasing the intersection angle between photometry and interferometry channels can improve the splitting ratio. Regardless, the spectral splittings are achromatic as required for the instrumental needs, as shown in 4.

At 3.75 μm, the centre wavelength of the L' band, the coupling ratios of the individual three couplers of each beam combiner as a function of interaction length are illustrated in Fig.5 (Plot 1, 2, 3, and 4). In the same figure, Plot 1 represents the coupling ratios of the DC1 and is labelled as dot-sign (Bar and Cross) and cross-sign (Bar and Cross) when the light is injected into Input 1 and Input 2 separately. Plot 2 shows the results for DC2 when the signal is injected into Input 3 and Input 4. Plot 3 and 4 show the same data for the CC using the same labels and colour. Bar and Cross-ratios are significantly off from 50/50 for the interaction lengths used for the directional couplers in the 4T beam combiners. To find the interaction length for 50/50 coupling, the same characterization procedure was employed for the reference 2 × 2 directional couplers on side B. The results are shown in Plot 5 and Plot 6 of Fig.5 for injection into the left and right input of the 2 × 2 directional couplers, respectively. The trend suggests that 50/50 coupling can either be achieved for shorter interaction lengths or longer interaction lengths than used for the directional couplers (DC1, DC2, and CC) in the 4T beam combiners. However, the splitting ratio of directional couplers with a long interaction length, i.e. 7.0 mm, is less chromatic compared to the directional couplers with a short interaction length.

6. INTERFEROMETRIC CHARACTERISATION

To investigate the contrast and extinction ratio or nulling depth, we chose the directional coupler with 7.0 mm interaction length from the block of reference 2 × 2 directional couplers (l = 4.0 mm to l = 7.0 mm) because

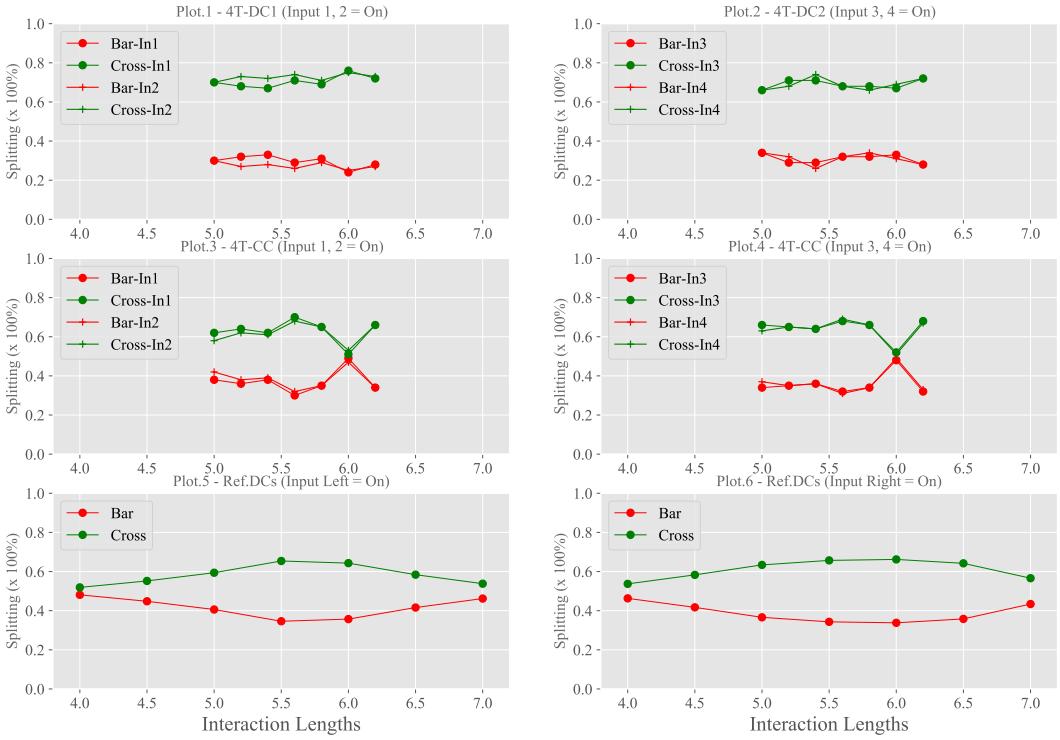

Figure 5. Coupling ratios at a wavelength of at 3.75 µm of the various directional couplers in the chip extracted from the Fourier Transform measurement. Plot 1, 2, 3, and 4 show the coupling ratios for the directional couplers in the 4T beam combiners as function of interaction length. In case of Input 1 and 2 (= On) indicates DC1, and corresponding CC is in operation while Input 3 and 4 (= On) indicates DC2, and subsequent CC is functioning. Plot 5 and Plot 6 represent the coupling ratios of the set of reference 2×2 directional couplers (DC) for injection into their left and right input, respectively.It is evident that the directional couplers of the 4T beam combiners to not meet the 50/50 splitting requirement and from the reference directional couplers it can be concluded that the interaction length can either be decreased or increase in order to achieve 50/50 splitting. It is noticeable that the CC with 6.0 mm interaction length is off from the trend, which is likely caused by defects related to a preexisting nucleation site or glass inhomogenity inside the GLS subtract.

it showed the least chromaticity and almost 50/50 splitting compared to the other directional couplers. The method employed to record the interferogram, called dynamic method (DM) has been previously described.[16] First the zero-OPD position is identified using the delay line and then the following steps are performed.

- Simultaneously injected the two beams of the Michelson interferometer, one into each input of the 7.0 mm long DC (Input 1 and Input 2).
- Optimizing one input to minimize the unbalance of output A.
- Recorded the interferogram with the help of delay line as IA when both beams were coupled to 2 inputs.
- Determined IA(max) and IA(min) from IA and subtracted with different background points, and then, Contrast, $C = I(max) - I(min)/I(max) - I(min)$ and Null Depth, $N = I(min)/I(max)$ are calculated which is the ratio between the destructive and constructive state of the interferogram.
- Separately, two photometric references were recorded by blocking input 2 for measuring I1A and input 1 as I2A.

- From the photometry, we calculated IA(max) as $IA(max) = (IA1)^2 + (IA2)^2 + 2\sqrt{IA1.IA2}$ and IA(min) as $IA(min) = (IA1)^2 + (IA2)^2 - 2\sqrt{IA1.IA2}$ and calculated C and N using previous equations.

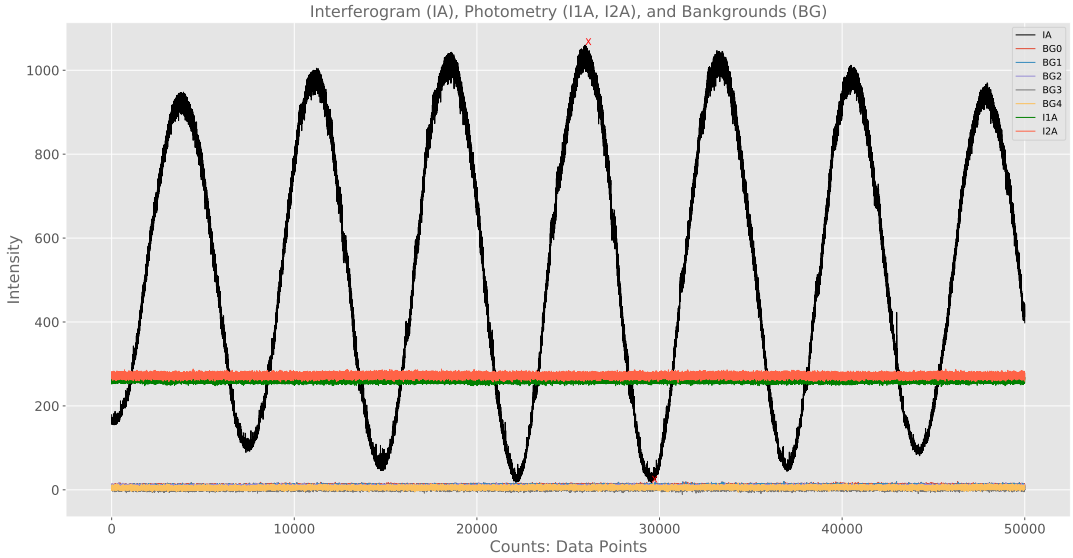

Figure 6. This graph shows an experimentally recorded interferogram (IA). The red crosses mark the maximum intensity, IA(max), and the minimum intensity IA(min). The background (BG) intensity taken from various points in the camera image are shown as BG0-BG4. IA1 and IA2 are the photometric taps.

The calculated results show that the experimental contrasts extracted from IA are 0.9734, with the black-body source and 0.9877 using the supercontinuum source. The theoretically estimated contrast using the photometry values, IA1 and IA2, are 0.999 for both sources. Hence, the corresponding null depths are in the 10^-2.

In practice, an average background signal from a point source from the surrounding area of the interferogram (IA) was chosen and subtracted from the null, IA(min). Using different background points provides different null values, as shown by the scattering of data points in Fig.6 for 8 independent measurements. The plot shows that all null depth are in the range of 0.03 or better. Further work is required to develop a reliable post-processing algorithm for determining the background count.

7. CONCLUSION

A prototype of the 4T nulling beam combiner for the Hi-5 instrument operating in the L' band was experimentally characterised. The integrated optic beam combiner is based on laser inscribed waveguides in a GLS glass subtract. The splitting characteristics of the building blocks of the beam combiner, such as Y-junctions and reference 2×2 directional couplers (DC), both showed achromaticity. The DC (7.0 mm) exhibited high contrast over the targeted wavelength band. High contrast and achromaticity are two key requirements of the Hi-5 instrument. The trend of splitting ratio of the directional couplers in the 4T beam combiner as a function of interaction length showed that they need optimisation in order to achieve 50/50 splitting. During the experiments it was found that the measured null-depths or extinction ratios of the directional couplers are highly dependent on the background. A reliable algorithm needs to be developed to determine the background during the interferometric experiments.

ACKNOWLEDGMENTS

AS, LL, and SG acknowledge the financial support by the Macquire University, Australia (iMQRES Scholership-20191092) and the Deutscher Akademischer Austauschdienst, Germany(DAAD Research Grants-57440920),

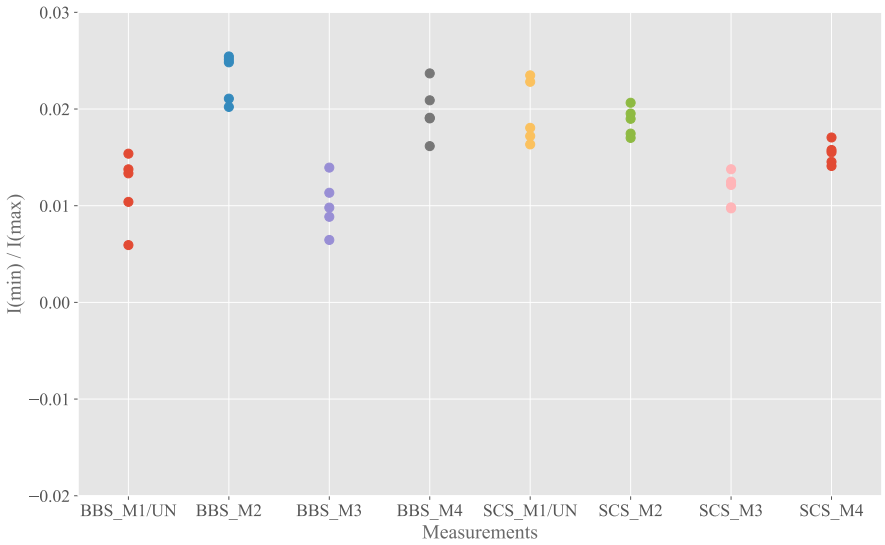

Figure 7. The null depth is dependent on the selection of the background signal. This plot shows the null depths for 8 independent measurements. These measurements were taken by following the dynamic method (DM), except BBS_M1 and SCS_M1. Those were manually taken without any input injection optimization or balancing output A to equalize IA1 and IA2.

through the Cotutelle agreement.

REFERENCES

[1] Defrère, D., Absil, O., Berger, J.-P., Danchi, W. C., Dandumont, C., Eisenhauer, F., Ertel, S., Gardner, T., Glauser, A., Hinz, P., et al., "Review and scientific prospects of high-contrast optical stellar interferometry," in [*Optical and Infrared Interferometry and Imaging VII*], **11446**, 387–405, SPIE (2020).

[2] Bracewell, R. N., "Detecting nonsolar planets by spinning infrared interferometer," *Nature* **274**(5673), 780–781 (1978).

[3] Angel, J. and Woolf, N., "An imaging nulling interferometer to study extrasolar planets," *The astrophysical journal* **475**(1), 373 (1997).

[4] Errmann, R., Minardi, S., Labadie, L., Muthusubramanian, B., Dreisow, F., Nolte, S., and Pertsch, T., "Interferometric nulling of four channels with integrated optics," *Applied Optics* **54**(24), 7449–7454 (2015).

[5] Defrère, D., Absil, O., Berger, J.-P., Boulet, T., Danchi, W., Ertel, S., Gallenne, A., Hénault, F., Hinz, P., Huby, E., et al., "The path towards high-contrast imaging with the vlti: the hi-5 project," *Experimental Astronomy* **46**(3), 475–495 (2018).

[6] Serabyn, E., Mennesson, B., Martin, S., Liewer, K., and Kühn, J., "Nulling at short wavelengths: theoretical performance constraints and a demonstration of faint companion detection inside the diffraction limit with a rotating-baseline interferometer," *Monthly Notices of the Royal Astronomical Society* **489**(1), 1291–1303 (2019).

[7] Martinache, F. and Ireland, M. J., "Kernel-nulling for a robust direct interferometric detection of extrasolar planets," *Astronomy & Astrophysics* **619**, A87 (2018).

[8] Norris, B. R., Cvetojevic, N., Lagadec, T., Jovanovic, N., Gross, S., Arriola, A., Gretzinger, T., Martinod, M.-A., Guyon, O., Lozi, J., et al., "First on-sky demonstration of an integrated-photonic nulling interferometer: the glint instrument," *Monthly Notices of the Royal Astronomical Society* **491**(3), 4180–4193 (2020).

[9] Labadie, L., Berger, J.-P., Cvetojevic, N., Haynes, R., Harris, R., Jovanovic, N., Lacour, S., Martin, G., Minardi, S., Perrin, G., et al., "Astronomical photonics in the context of infrared interferometry and high-resolution spectroscopy," in [*Optical and Infrared Interferometry and Imaging V*], **9907**, 322–342, SPIE (2016).

[10] Labadie, L., Minardi, S., Tepper, J., Diener, R., Muthusubramanian, B., Pott, J.-U., Nolte, S., Gross, S., Arriola, A., and Withford, M. J., "Photonics-based mid-infrared interferometry: 4-year results of the alsi project and future prospects," in [*Optical and Infrared Interferometry and Imaging VI*], **10701**, 516–531, SPIE (2018).

[11] Gross, S. and Withford, M., "Ultrafast-laser-inscribed 3d integrated photonics: challenges and emerging applications," *Nanophotonics* **4**(3), 332–352 (2015).

[12] Gretzinger, T., Gross, S., Arriola, A., and Withford, M. J., "Towards a photonic mid-infrared nulling interferometer in chalcogenide glass," *Optics Express* **27**(6), 8626–8638 (2019).

[13] Osellame, R., Cerullo, G., and Ramponi, R., [*Femtosecond laser micromachining: photonic and microfluidic devices in transparent materials*], vol. 123, Springer (2012).

[14] Ródenas, A., Martin, G., Arezki, B., Psaila, N., Jose, G., Jha, A., Labadie, L., Kern, P., Kar, A., and Thomson, R., "Three-dimensional mid-infrared photonic circuits in chalcogenide glass," *Optics Letters* **37**(3), 392–394 (2012).

[15] Arriola, A., Mukherjee, S., Choudhury, D., Labadie, L., and Thomson, R. R., "Ultrafast laser inscription of mid-ir directional couplers for stellar interferometry," *Optics Letters* **39**(16), 4820–4822 (2014).

[16] Tepper, J., Labadie, L., Diener, R., Minardi, S., Pott, J.-U., Thomson, R., and Nolte, S., "Integrated optics prototype beam combiner for long baseline interferometry in the l and m bands," *Astronomy & Astrophysics* **602**, A66 (2017).